certain training-set size (about 200 for the case in Fig. 2) beyond which the addition of further training samples effects network training but marginally.

In this communication we showed results of some experimentation with the ability of a neural network to estimate a multi-dimensional continuous function. The relationships between the network parameters (number of hidden neurons) and the complexity of the function to be estimated were found to be approximately linear for one complexity measure (the order) and faster than linear for another measure (the dimensionality). Our results will hopefully provide the designer of a neural-based system with an intuition about these relationships between errors that can be expected, complexity of a function and size of the network to use. Using some experimentation, the designer should be able to obtain approximate information concerning the complexity of his data. This will enable him to employ our results.

Our results support the conclusion that neural networks are indeed able to perform accurate regression on non-linear functions – in all cases studied suitable parameter choices could be found to reduce the rms error to below the 1% level. It is clear that the 'curse of dimensionality' will, however, eventually catch up with this technique (as with any known method of non-linear regression).

Several interesting questions remain to be studied, such as the extent to which noise rejection is possible; comparisons with other methods of non-linear regression should be made, and methods of dealing with the dimension explosion have to be found.

1. Huang W. and Lippmann R. (1988). Neural net and traditional classifiers. In *Neural Information Processing Systems*, ed. D.Z. Anderson, pp. 387–396. AIP, Denver, CO.
2. Khotanzad A. and Lu J. (1988). Distortion invariant character recognition by a multilayer perceptron and backpropagation learning. In *International Conference on Neural Networks*, pp. I-625–I–632. IEEE, San Diego, CA.
3. Barnard E., Cole R., Vea M. and Alleva F. (1991). Pitch detection with a neural-net classifie. *IEEE Trans. Sig. Proc.* **39** (2), 298–307.
4. Cherkassky V., Lee Y. and Lari-Najafi H. (1991). Self-organizing network for regression: efficient implementation and comparative evaluation. In *International Joint Conference on Neural Networks* pp. I-79–I-84. IEEE, Seattle, WA.

A chronological framework for colluviation during the last 110 kyr in KwaZulu/Natal

A.G. Wintle,[1] G.A. Botha,[2] S.H. Li,[3] and J.C. Vogel*

[1]Institute of Earth Studies, University of Wales, Aberystwyth, Dyfed, SY23 3DB, UK; [2]Council for Geoscience, P.O. Box 900, Pietermaritzburg, 3200 South Africa; [3]Radioisotope Unit, University of Hong Kong, Pokfulam Road, Hong Kong; and *QUADRU, Ematek, CSIR, P.O. Box 395, Pretoria, 0001 South Africa.

Luminescence dating techniques have been applied to colluvial sediments of the Masotcheni Formation at four sites in northern Natal. Details of the thermoluminescence (TL) and infrared-stimulated luminescence (IRSL) results are given, as well as measurements of the radioactive content of the samples. The results suggest that the feldspar grains were well enough bleached by sunlight at deposition to allow dating by IRSL techniques. The ages obtained suggest that colluvial deposition occurred during late Oxygen Isotope Stage 5, after the peak of the Last Interglacial (Sub-stage 5e), resulting in the Dingaanstad Alloformation. No colluvial deposits were recorded from Stage 4. Further colluvial deposition, represented by the Nqutu Allomember, seems to have commenced early in Stage 3, following a period of donga erosion. A soil was then formed during Stage 3 in the top of this deposit at two of the sites, and this was covered by more colluvial deposits before Stage 3 ended. Evidence for late Holocene colluviation is also presented.

Colluvial deposits occur extensively in northern Natal, although in most instances they are relatively thin and contain little stratigraphic information. However, in some areas colluvial deposits of up to 21 m thick have accumulated, through the action of sheet wash, soil creep and other mass-movement processes, within shallow bedrock depressions on footslopes at the base of sandstone- or dolerite-capped hills. The sedimentary succession, named the Masotcheni Formation,[1] comprises sandy colluvial sediments and a number of buried palaeosol profiles[2] exposed in erosion gullies (dongas) which are currently forming or extending. Several cycles of donga erosion, colluviation and palaeosol formation during the late Quaternary have been described by Botha *et al.*[3] and Botha,[2] with one of the most complex, and complete, records exposed in sidewalls of the Dabekazi donga near the St. Paul's Mission in northern Natal (Fig. 1).

The chronological history of the colluvial sediments exposed in the dongas throughout an area of 40 000 km^2 has been based on a small number of radiocarbon dates[3] and on correlation of sedimentary units and associated palaeosols on pedogenic characteristics, such as colour, structure and texture, and relative stratigraphic position. Concise descriptions of allostratigraphic subdivisions of the Masotcheni Formation are shown in Table 1 (from ref. 2). On the basis of poorly constrained archaeological evidence it has been proposed that these sediments accumulated within the last 100 kyr, after the end of the Last Interglacial (deep-sea Oxygen Isotope Sub-stage 5e).[3] The oldest sediments represent pedogenically preweathered material derived from erosion of soil profiles upslope, and deposited on fresh bedrock surfaces from which all traces of possible earlier sediments and soil profiles appear to have been removed by intense hillslope erosion or stream activity. Today such ephemeral streams are incising colluvia down to bedrock through the active erosion of dendritic donga systems.

At several sites, radiocarbon dates have been obtained for organic matter associated with clay in a distinctive dark grey, buried palaeosol 'marker unit', the Hazeldene Pedoderm. This palaeosol is developed within the reddish-brown Nqutu Allomember, part of a widespread colluvial complex, the St. Paul's Alloformation. At the sites where calcium carbonate nodules have been found within palaeosols of this unit, these have also been dated using radiocarbon.[3,5]

More recently, luminescence dating methods were applied to four samples from the Dabekazi donga wall near St. Paul's Mission.[4] These samples were dated using the infrared-stimulated luminescence (IRSL) signal from the silt-sized grains within the colluvium. Three of the samples were from the St. Paul's Alloformation and gave ages of 37 ± 3, 36 ± 3 and 36 ± 3 kyr (AF-3,

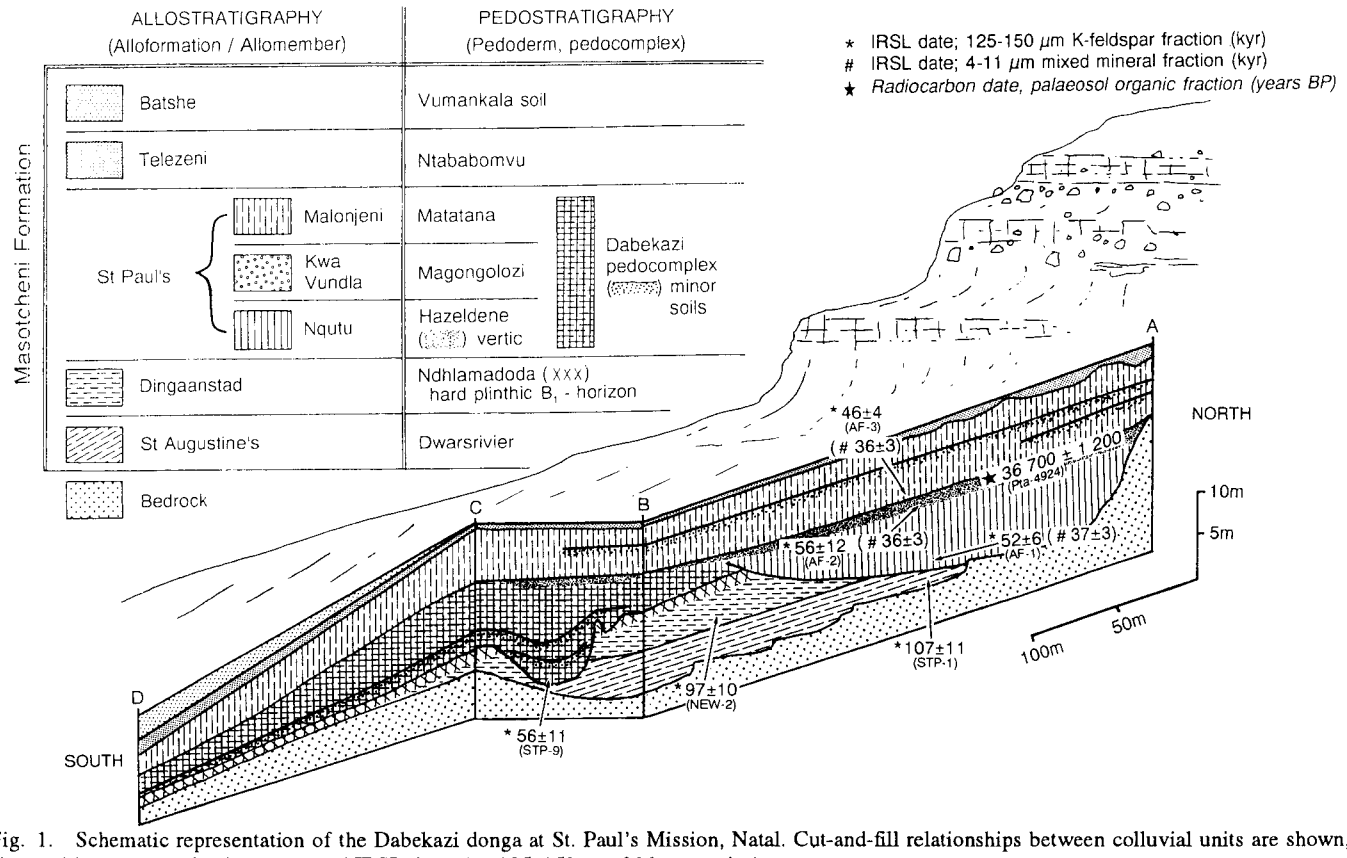

Fig. 1. Schematic representation of the Dabekazi donga at St. Paul's Mission, Natal. Cut-and-fill relationships between colluvial units are shown, along with positions of radiocarbon and IRSL dates (on 125–150-μm feldspar grains).

2 and 1 respectively, see Fig. 1). These were consistent with a radiocarbon age of 36 700 ± 1 200 yr BP (Pta-4924), which had been obtained on organic matter complexed onto clay in the buried Hazeldene Pedoderm at this site. However, the stratigraphic positions of these three samples caused Wintle *et al.*[4] to question the long-term stability of the IRSL signal from the mixed-mineral, fine grains (4–11 μm) used in the study. It was also considered possible that grains of this size could illuviate down through the sediment column after burial of the palaeosol.

Wintle *et al.*[4] reported an experiment in which greater thermal stability was shown for larger-grained feldspars (125–150 μm) separated using heavy liquid with a density of 2.58 g cm^{-3}. In this article we report dates obtained using this separated mineral fraction for a number of samples from the colluvial succession at St. Paul's Mission and other sites in KwaZulu/Natal, namely Nqutu, Masotcheni and Matatana.[2,5]

IRSL dating procedures

IRSL is the luminescence signal observed when feldspar grains are exposed to infrared photons after they have received a radiation dose. The natural IRSL signal (obtained from grains extracted from the sediment sample in very low light conditions) is produced as a result of exposure to ionizing radiation from the uranium and thorium decay chains and ^{40}K in the grains and their immediate environment. The amount of radiation to which the grains have been exposed since deposition (known as the equivalent dose, ED) can be determined by comparing the natural IRSL with IRSL signals induced by laboratory irradiation. The age of the sediment is given by the equation

$$\text{Age (yr)} = \frac{\text{Equivalent dose (Gy)}}{\text{Dose rate (Gy yr}^{-1})}$$

The dose rate is obtained by measuring the different radioactive components in the environment of the sediment. Further details can be found elsewhere.[6]

Table 1. Description of allostratigraphic subdivisions of the Masotcheni Formation, after Botha.[2]

Allostratigraphy (Alloformation/Allomember)		Allo-unit characteristics
Batshe Alloformation		Colluvial fan deposited prior to the incision of the current dongas
Telezeni Alloformation		Debris flow/ talus deposits fining downslope
St. Paul's Alloformation (comprises the thin, stacked colluvial units which infill palaeodongas incised into Dingaanstad Alloformation sediment)	Malonjeni Allomember	Yellow-brown sediment ubiquitous in donga exposures. Thickness variable and generally present even where older/ younger units are not present
	Kwa Vundla Allomember	Leached, sandy colluvium sometimes found overlying the Hazeldene Pedoderm but may overlap onto the adjacent, truncated Ndhlamadoda Pedoderm hard plinthite
	Nqutu Allomember	Red stratified colluvium deposited in steep-sided palaeodongas incised into Dingaanstad Alloformation sediments. The distinctive Hazeldene Pedoderm forms in the top of these sediments
Dingaanstad Alloformation		Reddish-brown stratified colluvium containing petroplinthite gravel
St. Augustine's Alloformation		Stratified colluvium preserved in bedrock hollows

ED determination

In order to investigate which measuring technique would best apply to these colluvial deposits, the EDs of the samples were measured in different ways. Both IRSL and thermoluminescence (TL) analyses were made on a Riso TL/OSL reader[7] fitted with infrared diodes for stimulation. IRSL and TL was observed with a 2-mm Schott BG-39 filter chosen for total rejection of the 880-nm IR from the diodes. For the TL measurements, the heating rate was 5°C s^{-1}. The blackbody radiation through the BG-39 was relatively low, as all the grains were very bright; the background run was nevertheless subtracted. For the brightest grains, a neutral-density filter was also employed. The 125–150-μm grain-size feldspar fraction was used throughout, in contrast to the fine-grain results mentioned above. About 4–8 mg was stuck to the 1-cm-diameter aluminium discs using silicon spray and all discs were normalized using the IRSL from a 0.1-s IR exposure before any further treatment.

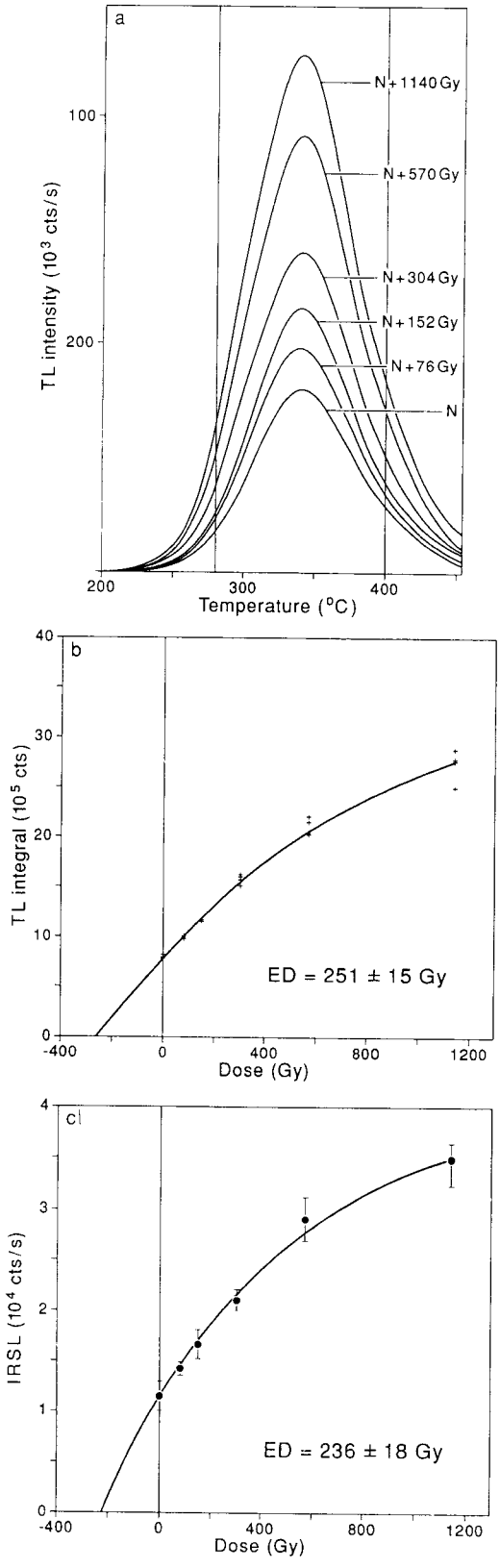

Fig. 2. Data for sample HIT-4. *a*, Thermoluminescence (TL) glow curves obtained for natural TL (N) and response to added doses as shown. Vertical lines show integral region used to obtain the equivalent dose (ED). *b*, TL growth curve using integrated signals from *a*, with residual level after 15-h bleach already subtracted from each data point. Individual points shown and exponential fit applied to obtain ED. c, IRSL growth curve obtained for the same discs used in *b*, with mean of six discs shown and exponential fit applied to obtain ED.

The three methods applied to these coarse-grain feldspars were:

i) The IRSL single-aliquot regeneration method, using a 1 600-s bleach with the diodes in the reader to zero the IRSL between irradiations. The IRSL was measured for 100 s at 50°C, following a 220°C preheat for 10 min. Details of these procedures are given in an earlier paper by Wintle *et al.*[4]

ii) The IRSL additive-dose multiple-disc procedure, in which aliquots are given different added doses to increase the IRSL signal. After irradiation the discs are stored for 24 h before being subjected to preheating at 220°C for 10 min. The discs are then stored for a further three days before the IRSL is measured for 0.1 s.

The measurements were repeated two or three months later to check for short-term fading. The EDs were found to agree with those obtained previously, indicating the lack of a short-term fading component in the IRSL.

iii) For all samples (excluding STP1), TL measurements were then made on the discs used in (ii), and the EDs derived from the integrated TL signal between 275° and 400°C. A typical set of TL glow curves (after background subtraction) is shown in Fig. 2*a*, and the resulting growth curve is shown in Fig. 2*b*. After the preheat, the glow curves resulted in a good ED plateau for the temperature region 275–400°C. Residual levels were obtained using three different bleaching times, namely, 10 min, 1.5 h and

Table 2. Thick-source alpha counting results of bulk samples (unsealed count rate) and U and Th concentrations calculated from the pairs count rate.

Sample	Count rate (ks cm^{-2})	Th (p.p.m.)	U (p.p.m.)	Sealed/ unsealed	Th/U
St. Paul's					
AF-3	1.50 ± 0.02	14.7 ± 1.90	8.23 ± 0.59	1.05	1.79
AF-2	1.19 ± 0.02	11.3 ± 1.60	6.63 ± 0.50	1.05	1.70
AF-1	1.35 ± 0.02	14.3 ± 1.80	7.07 ± 0.56	0.97	2.02
STP-9	1.22 ± 0.01	13.5 ± 1.20	6.24 ± 0.37	0.95	2.16
NEW-2	1.43 ± 0.02	20.9 ± 2.10	5.78 ± 0.63	1.00	3.61
STP-1	0.96 ± 0.01	11.1 ± 1.30	4.81 ± 4.02	1.00	2.31
Nqutu					
HIT-4	1.70 ± 0.03	21.3 ± 0.03	7.98 ± 0.87	0.98	2.67
HIT-1	1.01 ± 0.02	12.5 ± 1.90	4.79 ± 0.59	0.98	2.61
HIT-3	0.66 ± 0.01	7.29 ± 1.16	3.34 ± 0.36	1.00	2.18
Masotcheni					
NEW-4	1.08 ± 0.02	10.6 ± 1.80	5.95 ± 0.57	0.97	1.78
NEW-3	0.69 ± 0.01	6.54 ± 0.79	3.82 ± 0.25	0.97	1.71
Matatana					
NEW-1	0.96 ± 0.02	11.64 ± 1.60	4.57 ± 0.48	1.08	2.52

Table 3. Comparison of EDs obtained with IRSL and TL signals. The TL EDs are given for different SOL2 bleaching times.

		IRSL ED (Gy)		TL ED (Gy)		
Section	Samples	Single disc	Multiple disc	15 h	1.5 h	10 min
St. Paul's	AF-3†	201 ± 2	226 ± 4	282 ± 16	262 ± 16	210 ± 15
	AF-2	294 ± 4	298 ± 51	283 ± 18	273 ± 18	232 ± 16
	AF-1†	259 ± 4	256 ± 20	380 ± 15	366 ± 14	295 ± 13
	STP-9†	324 ± 5	299 ± 44	362 ± 29	-	289 ± 26
	NEW-2*	383 ± 6	519 ± 19	484 ± 38	472 ± 38	415 ± 34
	STP-1	429 ± 8	467 ± 24	-	-	-
Nqutu	HIT-4*	185 ± 3	236 ± 18	251 ± 15	240 ± 14	201 ± 14
	HIT-1†	226 ± 3	244 ± 4	290 ± 14	-	246 ± 13
	HIT-3*	233 ± 3	341 ± 13	304 ± 11	-	197 ± 12
Masotcheni	NEW-4	193 ± 2	202 ± 5	226 ± 12	205 ± 13	153 ± 14
	NEW-3†	423 ± 7	460 ± 8	575 ± 12	551 ± 12	447 ± 12
Matatana	NEW-1	364 ± 6	434 ± 27	456 ± 49	434 ± 48	338 ± 42

†Shows the samples for which the TL ED (using a 15-h bleach) is significantly larger than that obtained from the IRSL signal.

*Shows the samples for which the ED obtained by the multiple addditive dose method disagree with the ED obtained with the single-disc regeneration method.

15 h in the SOL2 solar simulator. Combining these with the additive-dose TL growth curve gave three values of ED.

The EDs obtained by these different techniques are listed in Table 3. The data points were fitted using a single exponential function, as illustrated in Figs 2*b* and 2*c*.

Comparison of TL and IRSL analyses

The TL EDs can be compared with those obtained from the IRSL measurements on the same set of discs. For NEW-1, NEW-2, HIT-3 and HIT-4 agreement can be seen between the TL EDs (15-h bleach) and the IRSL EDs from the multiple-disc method. This indicates that the grains were very well bleached at deposition. In addition the IRSL EDs from the single-aliquot approach for these samples were greater than 10% lower than those for the multiple-disc approach. This can be explained if bleaching with IR (during construction of the single-disc growth curve) erases the IRSL signal, but not the majority of the TL signal. Regeneration of discs bleached in this way would produce a larger IRSL signal and result in a lower ED.[9]

For AF-2 and NEW-4, the EDs for the TL (15-h bleach) and for both sets of IRSL measurements are similar. Again the samples were sufficiently bleached at deposition, to zero the IRSL and erase the most light-sensitive part of the TL signal.[10]

In contrast, samples AF-3, AF-1, NEW-3, HIT-1 and STP-9 give larger EDs with the TL method (15-h bleach) than with either IRSL approach. For these samples there is much better agreement of the IRSL EDs with the TL EDs for a much shorter bleaching time (10 min). These results suggest that the TL signal of these samples was probably not sufficiently erased during deposition.

Incomplete bleaching behaviour for this type of sediment was supported by studies on two samples taken from the Batshe Alloformation and the underlying Telezeni Alloformation at the top of the colluvial succession at the Dabekazi donga. The uppermost sample gave a minimum IRSL age estimate of 3.8 kyr and various tests implied that the grains were not well bleached at deposition; in particular, the TL age estimate was 25.7 kyr when a 10-min exposure in the SOL2 was used. For the sample from the Telezeni Formation, a best estimate of 1.8 ± 0.2 kyr was obtained, based on IRSL ages of 1.35 and 1.93 kyr, and the TL age of 1.92 kyr for the 10-min SOL2 exposure. These results are discussed in greater detail elsewhere.[11]

The above discussion leads us to the conclusion that, for the colluvial deposits discussed here, the most reliable dating will be obtained by using the EDs derived from the multiple-disc additive-dose IRSL method.

Dose-rate estimation

Thick-source alpha counting was used on ground bulk material, with measurements being made with the sample both unsealed and sealed against radon loss (Table 2). The listed count is that for the unsealed measurement. Samples were counted between one and eight weeks after grinding. (It should be noted that the alpha counting results are slightly different from the three given in the previous publication; the latter were obtained after they had been crushed in a ball mill, a procedure which was not available for the rest of the samples.) The Th and U p.p.m. values derived from the pair counts[6] are also given.

The potassium content of bulk samples was measured in an atomic absorption spectrometer. For the feldspar grains themselves a Geiger-Müller multicounter system was used.[12] The K_2O content for these samples was much lower than has been found for other separates from different regions of the world. The feldspar grains were crushed in a ball mill and about 0.4 g of material was alpha counted using 1.6-cm-diameter ZnS screens. The IRSL alpha efficiency was measured for NEW-3 as 0.15 ± 0.02 and this value was used for all samples.

The beta dose rate was measured using a thick-source beta counter (TSBC),[13] with 15 g of sample being used for each measurement. Table 4 shows the measured beta dose rate alongside those calculated from the alpha counting and potassium content measurements. The mean ratio of these beta counts is 0.93 ± 0.09 and the uncertainty in each beta dose rate is typically ± 0.2 Gy yr^{-1}. For calculation of the total dose rate, the beta dose rate, based on the alpha counting and K analysis were used.

For the age calculation, an estimate of the past water content (weight water/weight wet sediment) is entered into the programme (by R. Grün) and a value of 10 ± 5% was assumed for all

Table 4. Summary of dose-rate evaluation for feldspar fractions and the IRSL ages.

	Bulk sample				Feldspar grains				
			β dose rates(Gy kyr^{-1}						
Samples	α count (c ks^{-1} cm^{-2})	K_2O (%)	from β count	from α count and K_2O	α count (c ks^{-1} cm^{-2})	Int. dose rate excl. K* (Gy kyr^{-1})	K_2O (%)	Total dose rate (Gy kyr^{-1})	Age (kyr)
St. Paul's									
AF-3	1.50 ± 0.02	1.84	2.52	2.79	0.034	0.22	2.8	4.84 ± 0.38	46 ± 40
AF-2	1.19 ± 0.02	2.52	2.99	3.06	0.100	0.65	2.7	5.34 ± 0.37	56 ± 12
AF-1	1.35 ± 0.02	1.76	2.60	2.79	0.064	0.42	3.2	4.96 ± 0.37	52 ± 6
STP-9	1.22 ± 0.01	2.20	2.81	2.91	0.116	0.76	4.0	5.31 ± 0.35	56 ± 11
NEW-2	1.43 ± 0.02	2.00	2.51	2.44	0.087	0.57	4.9	5.35 ± 0.39	97 ± 10
STP-1	0.96 ± 0.01	2.32	2.91	2.67	0.046	0.30	2.0	4.38 ± 0.34	107 ± 11
Nqutu									
HIT-4	1.70 ± 0.03	2.16	2.86	3.19	0.036	0.23	8.0	5.78 ± 0.46	41 ± 5
HIT-1	1.01 ± 0.02	1.68	1.97	2.21	0.128	0.84	6.4	4.62 ± 0.34	53 ± 6
HIT-3	0.66 ± 0.01	1.72	1.90	1.93	0.052	0.34	7.8	3.56 ± 0.28	96 ± 10
Masotcheni									
NEW-4	1.08 ± 0.02	1.20	1.40	1.94	0.044	0.29	2.2	3.59 ± 0.32	56 ± 6
NEW-3	0.69 ± 0.01	1.56	1.48	1.85	0.072	0.47	3.0	3.40 ± 0.26	135 ± 14
Matatana									
NEW-1	0.96 ± 0.01	1.76	2.01	2.20	0.051	0.33	2.9	3.93 ± 0.32	110 ± 13

*Derived from α count rate and corrected for attenuation, but excluding the contribution from potassium.

samples. The cosmic ray contribution was calculated using the equation given in Prescott and Hutton.[14]

Discussion

The IRSL age estimates obtained using the above measurements are given in Table 4. The first point to note is that the ages obtained for AF-3, AF-2 and AF-1 (46 ± 4; 56 ± 12 and 52 ± 6 kyr, respectively) are significantly older than those obtained for the same samples but using the fine grains, namely, 37 ± 3; 36 ± 3 and 35 ± 3 kyr, respectively.[4] In this earlier study, the dates were thought to be consistent with the radiocarbon age for the palaeosol, but the similarity of the IRSL ages obtained for samples above (AF-3) and well below (AF-1) the palaeosol were unexpected. One explanation is the possible movement of fine grains (<10 μm) down through the section by percolating water.

Another explanation for the lower ages lies with the possibility that the signal from the fine grains is less thermally stable than that from the 125–150-μm fraction. The thermal response of the fine-grain fraction of AF-3 and the 125–150-μm feldspar separate for the same sample was compared in pulse-annealing experiments and it was concluded that the IRSL signal of the latter had greater thermal stability.[4] An additional experiment was carried out in which storage at 140°C for 18 h was found to reduce the IRSL signal of the fine grains to 67% of its initial value, and that of the larger grain size to 86% of its initial value. These results confirmed the conclusion of the previous experiment. Although this limited experimental programme cannot prove that thermal instability is the cause of the underestimation by the fine grains, it seemed prudent to use the coarse-grain signal. On the basis of either explanation, the previously obtained fine-grain dates should be replaced by those for the coarse-grain feldspars.

It must also be pointed out that the discrepancy between the radiocarbon date of 36 700 ± 1 200 yr BP (Pta-4924) and the immediately overlying IRSL date of 46 ± 4 kyr is actually not as great as it seems if one takes into account that radiocarbon dates in this age range are found to be several thousand years younger than the calendar date.[15]

St. Paul's Mission

The IRSL ages presented in this article suggest that the dark-grey Hazeldene palaeosol was formed in the top of the Nqutu Allomember just before 46 ± 4 kyr. STP-9 is from the base of an infilled palaeodonga seen in section B–C (Fig. 1) parallel to the current donga. Its age of 56 ± 11 kyr is similar to the date for AF-2 (56 ± 12 kyr) and AF-1 (52 ± 6 kyr) from an adjacent, obliquely incised palaeodonga infilled with the red sediment of the Nqutu Allomember. No samples were taken from the upper part of the St. Paul's Alloformation (i.e. above AF-3), which could have served to place a time limit on the duration of its accumulation. The numerous thin palaeosols formed within the sediment infilling of palaeodongas during this period suggest that the St. Paul's Alloformation records an unstable period on hillslopes in the region, with episodic erosion, colluviation and palaeosol formation. A best estimate of 1 770 ± 250 yr was obtained by IRSL for a sample (STP-13) taken from the Telezeni Alloformation.[11] This result shows that some deposition of colluvial sediment has taken place during the Holocene.

Two older colluvial/palaeosol units have been identified, namely the basal St. Augustine's Alloformation and the overlying Dingaanstad Alloformation, with dates for these units at St. Paul's provided by samples STP-1 (107 ± 11 kyr) and NEW-2 (97 ± 10 kyr), respectively.

Nqutu, Masotcheni and Matatana

The IRSL dates have been added to the schematic stratigraphy given in Table 5 and have been described elsewhere.[5] At Nqutu, the IRSL age for HIT-4 (41 ± 5 kyr) from a light-grey leached horizon at the base of the Malonjeni Allomember is not incon-

Table 5. Chronological framework based on IRSL and radiocarbon dates (kyr) for stratigraphic units comprising the Masotcheni Formation (adapted from Botha[2]). Afm = Alloformation; Amb = Allomember; Pdm = Pedoderm; italics = radiocarbon date. IRSL dates are from the 125–150-μm fraction.

Stratigraphy		St. Paul's	Nqutu	Masotcheni	Matatana
Batshe Alloformation		3.8			
Ntababomvu Pedoderm		*1.42 ± 0.06*			
Telezeni Alloformation		1.7 ± 0.2			
St. Paul's Alloformation	Malonjeni Amb	46 ± 4			
	Kwa Vundla Amb		41 ± 5		
	Hazeldene Pdm	*36.7 ± 1.2*	*24.6 ± 0.6*		
		56 ± 12			
	Nqutu Amb	52 ± 6	53 ± 6		
		56 ± 11			
	Unnamed palaeosol		*36.8 ± 1.2*		
Dingaanstad Afm		97 ± 10		56 ± 6	110 ± 13
St. Augustine's Afm		107 ± 11	96 ± 10	135 ± 14	

sistent with the age of 46 ± 4 kyr for sample AF-3 from the yellowish-brown Malontjenii Allomember at St. Paul's. The radiocarbon age of 24 600 ± 580 yr BP (Pta-4914) was derived from organic matter from the underlying Hazeldene Pedoderm, developed within red colluvium (Nqutu Allomember) for which an age of 53 ± 6 kyr (HIT1) was obtained, consistent with the same unit at St. Paul's Mission. It is possible that the organic matter could have been contaminated by the penetration of humic material from weakly developed soils in the overlying Malonjeni Allomember. Below the Nqutu Allomember a localized, unnamed organic-rich palaeosol was dated at 36 800 ± 1 200 yr BP (Pta-4928). Red colluvium below a boulder horizon at the base of the plinthic Ndlamadoda Pedoderm gave an age of 96 ± 10 kyr (HIT-3), which is in general agreement with the ages for the basal units at St. Paul's Mission.

At Masotcheni (10 km west of Nqutu, type site for the Masotcheni Formation), no organic-rich palaeosols have been found. Three colluvial units overly each other with a total maximum depth of 15 m.[2] NEW-3, taken at the base of the deepest part of the section, gave an age of 135 ± 14 kyr. NEW-4 from the overlying unit, identified as the Dingaanstad Alloformation,[2] gave an age of 56 ± 6 kyr, more consistent with the ages found for the stratigraphically younger Nqutu Allomember at the St. Paul's Mission site.

At Matatana one sample was collected (NEW-1) from the Dingaanstad Alloformation and gave an age of 110 ± 13 kyr, more consistent with the ages of the basal St. Augustine's Alloformation elsewhere. Recent evidence suggests that the NEW-1 sample might represent a thin truncated remnant of the older St. Augustine's Alloformation buried by Dinganstaad Alloformation sediment, the two generations of sediment effectively 'welded' by pedogenic features associated with the strongly developed Ndhlamadoda Pedoderm (ferricrete).

Conclusions

The IRSL age estimates suggest that the colluvial deposits of the Masotcheni Formation were deposited during the last 110 kyr, i.e. since the end of Oxygen Isotope Sub-stage 5e. So far, there is no evidence for colluvial sedimentation prior to the Late Pleistocene. The St. Augustine's Alloformation and the Dingaanstad Alloformation were probably formed during the period of Sub-stages 5d to 5b, but the error limits on the IRSL dates preclude their separation on the basis of age or their assignation to particular sub-stages. The next period of donga erosion followed by colluvial deposition occurred not earlier than 60 kyr, with the Nqutu Allomember being deposited rapidly around 56–50 kyr; soil-forming processes on its surface were initiated shortly thereafter. This was followed by further colluviation which started around 45 kyr, and continued for an unknown period, interrupted periodically by minor soil-forming processes, as clearly demonstrated on the donga wall at St. Paul's Mission. Therefore the lower units of the St. Paul's Alloformation were probably deposited during Stage 3. There is also evidence of Late Holocene deposition of colluvium.

Li was supported by a studentship provided by the Institute of Earth Studies. Luminescence dating of colluvial deposits has been supported by NERC grant GR9/644 and the Geological Survey of South Africa. This is publication 370 of the Institute of Earth Studies, prepared whilst the first author was on sabbatical leave at the CSIR, Pretoria.

Received 28 April; accepted 28 November 1994.

1. Davies O. (1976). The 'Sangoan' Industries. *Ann. Natal Mus.* **22**, 855–911.
2. Botha G.A. (1992). *The geology and palaeopedology of late Quaternary colluvial sediments in northern Natal, South Africa.* Ph.D. thesis, University of Natal.
3. Botha G.A., de Villiers J.M. and Vogel J.C. (1990). Cyclicity of erosion, colluvial sedimentation and palaeosol formation in Quaternary hillslope deposits from northern Natal, South Africa. *Palaeoecol. afr.* **19**, 195–210.
4. Wintle A.G., Li S.H. and Botha G.A. (1993) Luminescence dating of colluvial deposits from Natal, South Africa. *S. Afr. J. Sci.* **89**, 77–82.
5. Botha G.A., Wintle A.G. and Vogel J.C. (1994). Episodic late Quaternary paleogully erosion in northern KwaZulu/Natal, South Africa. *Catena* **23**, 327–340.
6. Aitken M.J. (1985). *Thermoluminescence Dating.* Academic Press, London.
7. Botter-Jensen I.,, Ditlefsen C. and Mejdahl V. (1991). Combined OSL (infrared) and TL studies of feldspars. *Nucl. Tracks Radiat. Measmt.* **18**, 257–263.
8. Li S.H. (1992). *Development and application of stimulated luminescence dating methods for sediments.* Ph.D. thesis, University of Wales, Aberystwyth.
9. Li S.H. and Wintle A.G. (1993). A model for sensitivity change of IRSL signals. *Ancient TL* **11**, 33–35.
10. Wintle A.G. and Huntley D.J. (1980). Thermoluminescence dating of ocean sediments. *Can.. J. earth Sci.* **17**, 348–360.
11. Wintle A.G., Li S.H., Botha G.A. and Vogel J.C. (1995). Evaluation of luminescence dating procedures applied to Holocene colluvium near St Paul's Mission, Natal. *The Holocene* **5**, 97–102.
12. Botter-Jensen L. and Mejdahl V. (1985). Determination of potassium in feldspars using a GM multicounter system. *Nucl. Tracks Radiat. Measmt.* **10**, 663–666.
13. Sanderson D.C.W. (1988). Thick source beta counting (TSBC): a rapid method for measuring beta dose rates. *Nucl. Tracks Radiat. Measmt.* **14**, 203–207.
14. Prescott J. R. and Hutton J.T. (1988). Cosmic ray and gamma ray dosimetry for TL and ESR. *Nucl. Tracks Radiat. Measmt.* **14**, 223–227.
15. Vogel J.C. (1983). ^{14}C Variations during the Upper Pleistocene. *Radiocarbon* **25**, 213–218.